

# Anomalous Frictional Behavior in Collisions of Thin Disks

John Calsamiglia  
Helsinki Institute of Physics  
Laser Physics and Quantum Optics Project  
FIN-00014 Helsingin Yliopisto, Finland

Anindya Chatterjee  
Engineering Science and Mechanics  
Penn State University  
University Park, Pennsylvania 16802

Scott W. Kennedy<sup>1</sup>  
Theoretical and Applied Mechanics  
Cornell University  
Ithaca, New York 14853

Andy L. Ruina  
Theoretical and Applied Mechanics  
Cornell University  
Ithaca, New York 14853

James T. Jenkins  
Theoretical and Applied Mechanics  
Cornell University  
Ithaca, New York 14853

Submitted to Journal of Applied Mechanics, July, 1997.  
Review suspended and revision requested: March 15, 1998.  
Revised and resubmitted: August 3, 1998

<sup>1</sup>Now at Division of Applied Sciences, Harvard University

## Abstract

We report on 2D collision experiments with 9 thin Delrin disks with variable axisymmetric mass distributions. The disks floated on an air table, and collided at speeds of about 0.5 to 1.0 m/s with a flat-walled stationary thick steel plate clamped to the table. The collision angle was varied. The observed normal restitution was roughly independent of angle, consistent with other studies. The frictional interaction differed from that reported for spheres and thick disks, and from predictions of most standard rigid-body collision models. For “sliding” 2D collisions, most authors assume the ratio of tangential to normal impulse equals  $\mu$  (friction coefficient). The observed impulse ratio was appreciably lower: roughly  $\mu/2$  slightly into the sliding regime, approaching  $\mu$  only for nearly grazing collisions. Separate experiments were conducted to estimate  $\mu$ ; check its invariance with force magnitude; and check that the anomalies observed are not from dependence on velocity magnitude. We speculate that these slightly anomalous findings are related to the 2D deformation fields in thin disks, and with the disks being only “impulse-response” rigid and not “force-response” rigid.

# 1 Introduction

Although the prediction of the outcome of collisions of approximately rigid bodies is of use for many purposes, there is not much collisional data on which to base or test predictive laws. Stoianovici and Hurmuzlu (1996) showed that for an apparently simple system, steel rods hitting an anvil, the collisional interaction is more complex than can be captured with known simple rigid body collision laws. Towards the end of better understanding basic issues, we set out to test collisions of an even simpler system, one for which the collisional mass matrix is diagonal (a “central collision”) and were surprised to find that even for this system some common rigid body collision assumptions are not applicable.

## 2 Sliding Collisions in 2D

We define here some sliding-related terms for 2D, frictional, single-point collisions: (1) In a *sliding* collision, the tangential components of pre- and post-collision relative velocity at the contact point are both nonzero and in the same direction. (2) In ‘single-point’ collisions, actual contact occurs over a small region. The *contact region* at any instant is the region occupied by the material points (on the two bodies) that are in contact at that instant. (3) At all times during a *fully sliding* collision, all points in the contact region have a nonzero relative tangential velocity in the same direction as the pre-collision relative tangential velocity. (4) A sliding collision that is not fully sliding is *partially sliding*.

In collisions of real objects it is possible that some portions of the contact region might stop or reverse their tangential velocity for part of the collision, yet *resume* sliding in the original direction by the end of the collision when all transient deformations are dead. Such a collision would naturally be partially sliding. If the frictional contact is governed by Coulomb friction, then the ratio of tangential impulse to normal impulse in a sliding collision will be less than  $\mu$  *only if* the collision is partially sliding.

Our definition of partial sliding is more macroscopic than that used by some authors. For example, in Mindlin and Deresiewicz (1953), partial sliding corresponds to some portions of the contact region sticking while others slip. In our experiments we can only distinguish between collisions where the ratio of tangential to normal impulse is roughly equal to  $\mu$  (treating them as fully sliding) from collisions where that ratio is convincingly less than  $\mu$  (treating them as partially sliding). We do not know the details of which parts of the contact surface are or are not sliding.

Predictions for general 3D frictional single-point collisions vary from model to model. However, for sliding collisions, if there is no inertial coupling between the normal and tangential directions<sup>1</sup> (as for collisions of axisymmetric disks or spheres with rigid walls), practically *all* authors assume the tangential impulse transmitted in the collision opposes the tangential velocity and is equal to  $\mu$  times the normal impulse. This is equivalent to assuming that central, sliding collisions cannot be partially sliding (this is one main point of this paper: our data shows that they can). Some more general rigid body collision models also explicitly or implicitly disallow partially sliding collisions. In Routh’s (1897) model for example, the ‘contact point’ has a unique tangential relative velocity at all times during the collision; in 2D, if the tangential relative velocity ever becomes zero during the collision, then it must either stay zero or reverse direction (by Routh’s model). Thus partial sliding is explicitly disallowed in 2D. In the models of Whittaker (1944), Kane and Levinson (1985), Smith (1991), and in the treatment of disk collisions by Brach<sup>2</sup>(1991), it is assumed that the ratio of impulses in a 2D sliding collision is

---

<sup>1</sup>Such collisions are sometimes called “central collisions”.

<sup>2</sup>Brach’s (1991) approach, in its most general form, suggests that the impulse ratio be treated as a tangential collision parameter that is not constant over all collisions between a given pair of bodies but that depends on initial conditions, e.g., the incidence angle. This approach is therefore neither supported nor contradicted by our data. Brach’s claims about planar collisions with Coulomb friction being either fully sliding or terminated at a ‘rolling’ condition are contradicted by our data.

always equal to the friction coefficient (thus partial sliding is implicitly disallowed). In the treatment of collisions of thick disks by Maw *et al.* (1981), based on the incremental contact analysis of Mindlin and Deresiewicz (1953), partial sliding is not disallowed *a priori*. The solution, however, predicts an impulse ratio of  $\mu$  for all sliding collisions (and some that are ‘almost’ sliding). The same occurs for disk collisions modeled using *ad hoc* localized compliances along the normal and tangential directions, as in Stronge (1994a). In the new algebraic rigid body collision model presented in Chatterjee and Ruina (1998b), it is possible to predict partially sliding disk collisions for suitable choices of the tangential restitution parameter  $e_t$ . However, that model also does not capture the present data with a single value of  $e_t$  for any one disk over the range of collision angles.

### 3 Description of Experiments

We now describe the disks studied and the experiments conducted (for more details, see Chatterjee, 1997).

#### 3.1 Disks

All nine disks were cut from a rod of Delrin stock<sup>3</sup> and finished on a lathe to achieve a smooth surface. The edge of each disk was rounded to ensure ‘point’ contact (see Fig. 1). Three of the disks had holes in their centers, and four disks had smaller aluminum disks glued to their centers. The disks were blackened and marked with two white dots: one near the edge and one at the center. The disks with holes in them had thin circular pieces of paper stuck to their lower faces to help them float on the air table. Table 1 outlines the properties of each disk. Note that disk pairs (1,2), (4,5) and (6,7) were made very similar (nearly identical) as a consistency check.

#### 3.2 Procedure

The disks moved on an effectively frictionless<sup>4</sup> air table and collided against a steel plate clamped to the air table. The plate (40.6 cm  $\times$  20.3 cm  $\times$  1.9 cm), about 130 times more massive than the most massive disk, is treated as infinitely massive in the analysis. Pictures of the moving disks were taken using a strobe lamp and a digital camera<sup>5</sup>. The strobe rate was held at about 8.8 Hz. This rate provided two to three images of the disk before and after each collision on one frame. The measurement precision was about 0.23 mm/pixel determined by number of pixels in digital camera, lens focal length and distance of camera from table surface (we made no checks of possible lens distortion errors). The launch speed of the disks was kept roughly consistent by using a simple rubber-band powered launcher, which also released the disks approximately without initial spin.

#### 3.3 Kinematic Measurements

Digital pictures of each collision were downloaded from the Kodak DCS and kinematic data was retrieved using the software *NIHImage*<sup>6</sup>. For each collision, we used four positions of the disk: two before and two after the collision. For each position, the  $x$  and  $y$  coordinates of the two marker points on the disk were recorded. Each set of coordinates (before, and after) was used to calculate the linear and angular velocities of the disk, before and after the collision.

---

<sup>3</sup>General Properties: low moisture absorption, abrasion resistance, dimensional stability and toughness, easy to machine.

<sup>4</sup>Based on the constancy of velocity and angular velocity before collision, the frictional effects were not greater than our measurement inaccuracy.

<sup>5</sup>Nikon F3 with attached Kodak Professional DCS (Digital Camera System).

<sup>6</sup>Available via anonymous ftp at [zippy.nimh.nih.gov](http://zippy.nimh.nih.gov)

### 3.4 Calculations

The quantities calculated for each collision were (1) the normal and tangential components of the pre- and post-collision velocities of the *contact point*, (2) the angle made by the pre-collision contact point velocity with the plate edge normal, (the ‘incidence angle’  $\theta$ ), (3) the coefficient of normal restitution  $e$  (ratio of normal separation velocity to normal approach velocity)<sup>7</sup>, (4) the ‘tangential restitution coefficient,’ defined here as the negative of the ratio of post-collision to pre-collision tangential contact point relative velocity, (5) the collision impulse from the steel plate to the disk, and (6) the ratio of the tangential to the normal components of the impulse (the ‘impulse ratio’).

### 3.5 Note on Error Bars

The error bars shown in the figures indicate estimated *upper bounds* on the errors in the plotted quantities. These bounds were obtained as follows.

For each collision, the measured quantities were the  $x$  and  $y$  coordinates of 8 points, i.e., 16 scalar quantities. Each calculated quantity, such as the coefficient of restitution or the angle of incidence, is thus a scalar function of 16 variables. For a function  $f(q_1, q_2, \dots, q_n)$ , if the measured quantities  $q_1, q_2, \dots, q_n$  have errors  $\Delta q_1, \Delta q_2, \dots, \Delta q_n$ , then the error in the calculated value of  $f$  is given to first order by the expression

$$\Delta f \approx \frac{\partial f}{\partial q_1} \Delta q_1 + \dots + \frac{\partial f}{\partial q_n} \Delta q_n = \nabla f \cdot \Delta \mathbf{q}.$$

Now each of the  $\Delta q_i$  would typically be about one pixel or less (the precision of the digital imaging system). However, we took the error to be about two pixels. From this, we obtain the estimated error bound

$$|\Delta f| \leq \sum \left| \frac{\partial f}{\partial q_i} \Delta q_i \right| \leq h \sum \left| \frac{\partial f}{\partial q_i} \right|,$$

where  $h$  is *twice* the data acquisition precision (length/pixel).

In the foregoing analysis, we neglected plate misalignment errors. We assume negligible error in the plate’s flatness, because the edge was machined flat specifically for the experiment. The surface normal was estimated by picking off the positions of two previously marked points on the plate edge. These points were about 880 pixels apart in the digital camera; incorrectly locating them by, say, 2 pixels corresponds to an error in estimating the normal direction by about .0023 radians (or less). The plate edge was also located separately for each picture, so the systematic error was probably even smaller. The horizontal error bars in the plots are several times bigger than 0.0023 even near grazing incidence, and still larger in other places. So plate misalignment error does not contribute substantially. In any case, since the plate was used to select axes, if the plate angle was off by a small amount, then the ‘true’ coordinates would change by correspondingly small amounts given by a rotation of axes formula. As such, the error from incorrectly orienting the plate is equivalent to incorrectly estimating the positions of various points, by amounts comparable to pixel size.

## 4 Results

For perfectly axisymmetric disks, all contact points are identical. Based on previous studies of disk and sphere collisions at moderate velocities (such as Maw *et al.* (1981) and Foerster *et al.* (1994)), we expect nondimensional collision quantities like the normal restitution coefficient  $e$  to be roughly independent of the pre-collision contact point velocity magnitude. Consequently, for a given disk, each

---

<sup>7</sup>There are other ‘definitions’ of the coefficient of restitution (see e.g., Smith and Liu (1992)), but the popular ones are equivalent for central collisions.

collision is approximately characterized by the incidence angle  $\theta$  alone. Quantities of interest in collisions of axisymmetric objects like disks are the normal restitution coefficient  $e$  and the ratio of tangential to normal impulse. Also of interest is the coefficient of tangential restitution, particularly for small incidence angles. We now present these quantities for the different disks, plotted against the incidence angle  $\theta$ .

#### 4.1 Normal Restitution

We found  $e$  to be fairly high (typically between about 0.92 and 0.96), roughly independent of  $\theta$ , and roughly the same for all 9 disks. This was as expected from the literature on experiments with thick disks (e.g., Maw *et al.*, 1981) and spheres (e.g., Foerster *et al.*, 1994). The results for disks 1 and 2 are shown in Fig. 2, and are representative of all 9 disks. The single data point at  $e \approx 1.08$  is interesting because it is greater than 1, though perhaps not convincingly so (given our error estimates). We mention that there is no fundamental reason why  $e$ , as defined in this paper, cannot be greater than 1 in *frictional* collisions (Smith and Liu (1992) report values as high as 2.3 from FEM simulations, and as high as 1.4 from experiments). See, e.g., Chatterjee and Ruina (1998b) for a discussion about the relation between  $e >, =, < 1$  and fundamental restrictions on collisional impulses.

#### 4.2 Tangential Restitution

We define the *tangential restitution coefficient* here as for normal restitution, as the negative of the ratio of post-collision tangential velocity to pre-collision tangential velocity. This ratio depends on  $\theta$ , and is shown for three pairs of disks in Fig. 3. In the figure, positive tangential restitution corresponds to tangential velocity reversal, which is not allowed by some rigid body collision models such as in Routh (1897), Whittaker (1944) or Kane and Levinson (1985). Tangential restitution effects, caused by tangential compliance effects, have previously been observed experimentally (Maw *et al.*, 1981; Foerster *et al.*, 1994). Observe that, as expected, the tangential restitution is roughly consistent between the nominally identical disks: between disks 1 and 2, disks 4 and 5, and disks 6 and 7. However, there is less consistency across disk pairs, and so the different disks have different tangential restitution graphs. For all disks (including the three remaining ones not shown for reasons of space) and  $\theta > \approx 0.5$ , all collisions were sliding. That all collisions for these disks should be sliding beyond  $\theta \approx 0.5$  is not predicted by any existing theory that we know of.

#### 4.3 The Impulse Ratio

The observed ratio of tangential to normal impulse is shown in Fig. 4. In each case, it is seen that the impulse ratio increases steadily with  $\theta$ , approaching about 0.16 in the limit of grazing incidence. Figure 5 shows the impulse ratio for *all* 9 disks on the same plot (without error bars for easier visibility). The degree of consistency between the data for the 9 non-identical disks is worth noting. The data can be fairly well captured using, say, a bilinear fit, with a corner at slightly under  $\theta = 0.5$ . As mentioned above, that is roughly where the transition occurs from tangential velocity reversal to sliding collisions.

In the sliding range, the impulse ratio is not constant but varies by roughly a factor of 2 as  $\theta$  goes from 0.5 to  $\pi/2$ . This variation is directly opposed to the usual predictions of standard rigid body collision models as well as a detailed solution by Maw *et al.* (1981). For comparison, the predicted impulse ratios for the cases of Routh’s law (1897), Kane and Levinson’s law (1985) (essentially the same as Whittaker (1944)), and Smith’s law (1991), using  $e = 0.92$ , for a uniform disk, and using a fitted coefficient of friction  $\approx 0.162$ , are plotted against incidence angle  $\theta$  in Fig. 5. The experimental data is represented by a bilinear curve. Note the mismatch of the bilinear fit to our data with the predictions of the conventional laws. We remark that as per several rigid body collision models, the ‘knee point’

marking the transition from tangential velocity reversal to sliding, in collisions of disks with rigid walls, occurs at an incidence angle that depends on the coefficient of friction, normal and tangential restitution behavior, as well as the radius of gyration. Since the radii of gyration of the disks were different (see the last column of table 1) while contact conditions were approximately the same, one might expect these knee points to occur at different incidence angles for these disks (which is apparently not the case; see Fig. 5). The typically predicted knee point for a uniform disk is far from that observed here (see Fig. 5).

## 5 Subsequent Experiments

### 5.1 Validity of the Coulomb Friction Contact Model

A year after the collision experiments we conducted some experiments to check the validity of the Coulomb friction model for the frictional interaction between the disks and the steel plate.

The original steel plate was lost, so we used another, similar plate. The coefficient of friction between the Delrin disks and the second plate was about 0.18. For the second plate, a pair of disks held side by side next to each other were attached together, constraining them to prevent rotation. Different steady normal loads were applied on them, and the tangential force needed to maintain sliding was measured. Within experimental precision, the sliding coefficient was found to be independent of normal force magnitude over about one order of magnitude. We can thus talk about ‘the’ coefficient of friction, in that Coulomb friction apparently described the contact interaction quite well, with a single friction coefficient  $\mu$  that is not dependent on the magnitude of the normal pressure.

For not-near-grazing collisions *impact data* does not allow an easy way to measure a friction coefficient. At other than grazing incidence, not all portions of the contact region may be sliding at any given instant. If the impulse ratio for near-grazing incidence is taken to be ‘the’ coefficient, then our data (Fig. 4) for the first plate gives our estimate of about 0.16. Microscopic determination of the shear and normal tractions acting over the contact region and of where and when points of contact were slipping would require more sophisticated local measurements than we could make in this limited study. Thus, more direct measurement of the friction coefficient acting during collision was not possible for these experiments.

### 5.2 Possible Velocity Dependence of the Impulse Ratio

In our experiments, the velocity magnitude was roughly constant while the incidence angle  $\theta$  was varied. Therefore, the normal component of collision velocity was roughly proportional to  $\cos \theta$ , i.e., a function of incidence angle. We would have liked to conduct similar experiments where the normal component of velocity was kept constant over all  $\theta$ . We were unable to conduct such experiments due to our inability to launch the disks accurately at arbitrarily specified speeds.

Possible dependence on normal velocity magnitude was investigated by studying a few more collisions of disk 2 with the new (second) plate. In these collisions, the incidence angle was held roughly constant while the magnitude of pre-collision velocity was changed (two sets of collisions, one at roughly 0.5 m/s and the other at roughly 0.9 m/s). Figure 5 shows the results obtained, compared with the previous measurements for that disk. It is seen that changing the velocity magnitude by a factor of about 1.8 apparently changes the average impulse ratio by only a slight amount (smaller than the inherent scatter in the data points themselves). The new data points for both velocity magnitudes lie a little higher than the old data points, by an amount roughly equal to the estimated difference in the coefficients of friction for the two plates (supporting an estimate of  $\mu \approx 0.16$  for the first plate and our measurement of  $\mu \approx 0.18$  for the second plate).

Moreover, the new data points for both speeds lie below the estimated limiting value for grazing incidence (i.e., 0.18). Thus, the data points for each speed corroborate the increasing trend in the impulse ratio seen in the first series of experiments.

We remark that the new data points for the lower speed (0.5 m/s) lie slightly higher, on average, than those for the higher speed (0.9 m/s). While not conclusive, this observation is consistent with theory in that for disks of fixed thickness and rounded edges, as the incidence velocity magnitude is made smaller and smaller, the localized 3D Hertz contact based solution (Maw *et al.*, 1981; Mindlin and Deresiewicz, 1953) is expected to become accurate: for sufficiently small velocity magnitudes, the impulse ratio graph is expected to be flat in the sliding regime.

### 5.3 Significance of Subsequent Experiments

The subsequent experiments described in this section roughly demonstrate two things. First, they show that a constant  $\mu$  is reasonable for the contact friction. By the discussion in Section 2, this implies that except in the limit of grazing incidence, the sliding collisions observed were only partially sliding collisions and not fully sliding collisions.

Second, and somewhat less conclusively, the velocity variation experiments indicate that dependence of the impulse ratio graph on pre-collision velocity magnitude is small. This constancy is consistent with the usual collision modeling assumption that collisional impulses are homogeneous of degree one in the velocities (impulse is linear with velocity magnitude, for fixed values of collision “parameters” such as restitution coefficients).

## 6 On Rigidity in Collisions

The fundamental assumptions of rigid body collision modeling are that the time of interaction is small, displacements during the collision are small, contact forces are large, and accelerations are large; that the net interaction can be described by rigid body impulse-momentum relations. Further, for ‘single-point’ collisions, it is assumed that the size of the contact region is small compared to the overall dimensions of the colliding objects. These assumptions are reasonably applicable for the disks studied. However, specific rigid body collision models include extra hypotheses about the collision impulse. The particular assumptions made vary; so do the predicted results. The contradiction between our experimental observations and the predictions of most standard rigid body collision models should be viewed as a demonstration of the weakness of specific assumptions of these particular collision models, and not inaccuracy of the fundamental assumptions of the rigid body approach.

In a collision between any pair of real objects, contact occurs over a region (possibly small). The velocity distribution of material points in the contact region need not be uniform. Apparently also, the common assumption of a constant  $\mu$  in the contact region is reasonable. If the relative tangential motion of all portions of the contact region is always in the same vectorial direction (with possible reversals), *and* the net tangential impulse is less than  $\mu$  times the normal impulse, then some portions of the contact region must have stuck or reversed direction for some part of the collision, even though the whole contact region might again be moving in the original direction at the end of the collision.

If contact deformations are strongly localized, as in (say) Hertzian contact of spheres or thick slices thereof, then the whole body moves essentially like a rigid body while the contact region acts like a small, pseudostatic interaction mechanism. Such objects, where at all instants of time including during the collision, the small contact region essentially behaves like a point on an ideal rigid body, are *force-response rigid* (see Chatterjee, 1997; or Chatterjee and Ruina, 1998a). Since any tangential (possibly rate-dependent) compliance is of the same order as normal compliance, these objects are expected to be slipping over the whole contact area throughout the collision for collisions that are sufficiently far

from normal. For such objects, in 2D sliding collisions, the tangential impulse is expected to be  $\mu$  times the normal impulse.

In contrast, if contact deformations are not so strongly localized, so that the motions of points at small distances from the contact region are *not* effectively identical to those of a point on a rigid body during the collision, but the motion of the body *before* and *after* the collision looks like that of a rigid body, and if all displacements during the collision are very small compared to the dimensions of the body, then the body is only *impulse-response* rigid (see Chatterjee (1997) or Chatterjee and Ruina (1998a)). In this case much more complex contact interactions can take place involving vibration and wave phenomena. Perhaps with such interactions the tangential relative velocity might reverse direction or stop during a collision (just as the normal component reverses direction multiple times in the data of Stoianovici and Hurmuzlu, 1996). For such objects, in 2D sliding collisions, it might happen that the tangential impulse is less than  $\mu$  times the normal impulse. As discussed in Chatterjee and Ruina (1998a) thin disks like in our experiments might only be well described as impulse-response rigid, while thick disks (as in Maw *et al.* (1981) might be well described as force-response rigid. In particular consider a slice of thickness  $H$ , cut from a sphere of radius  $R$ . Then the 3D Hertz-contact compliance (see Johnson, 1985) due to the rounded edges depends only on  $R$  and not on  $H$ , but the 2D compliance (or the ‘thinness’ effect of the disk) is proportional to  $1/H$ . For a given contact force magnitude, if  $H$  is made smaller, the two (3D and 2D compliances) can become comparable.

Note that the data of Foerster *et al.* (1994) and Maw *et al.* (1981) clearly showed tangential restitution, like our disks. Thus, our observations are not new in this regard. However, for the spheres and (presumably thick) disks studied in these works, it was found that the impulse ratio was equal to the friction coefficient for sliding collisions, i.e., in those studies, sliding collisions were fully sliding. In contrast, in our study of thin disks, we have found sliding collisions to be only partially sliding.

## 7 Conclusions

The fact that even in apparently “sliding” collisions, sliding need not persist *throughout* the collision, is relevant to general rigid body collision modeling. Contradiction of specific collision models, however, does not negate the basic rigid body approach to modeling collisions. We hope that our results will help to broaden the often restricted ideas about rigid body collisions that are promoted, in part, by several recent papers devoted to analyses of Routh’s incremental model or variations thereof, examples of which include Keller (1986), Wang and Mason (1992), Stronge (1994b), Bhatt and Koechling (1995), Marghitu and Hurmuzlu (1995) and Batlle and Cardona (1997).

The details of the actual mechanical interactions in the disk collisions studied here were not resolvable at our scale of measurements. These interactions might be better understood through some combination of experiments with micromasurements, detailed numerical simulations, and approximate analytical solutions.

## 8 Acknowledgements

The authors thank Michel Louge for the loan of the digital camera system, the National Science Foundation (REU program) for summer support for (then undergraduates) Calsamiglia and Kennedy, and the Department of Energy (Granular Flow Advanced Research Objective) for one summer’s support for Chatterjee.

## References

- [1] Batlle, J. A. and Cardona, S. The jamb (self-locking) process in 3D rough collisions. *ASME Journal of Applied Mechanics*, 65:417–423, 1998.
- [2] Bhatt, V. and Koechling, J. Three-dimensional frictional rigid-body impact. *ASME Journal of Applied Mechanics*, 62:893–898, 1995.
- [3] Brach, R. M. *Mechanical Impact Dynamics: Rigid Body Collisions*. John Wiley and Sons, New York, 1991.
- [4] Chatterjee, A. *Rigid Body Collisions: Some General Considerations, New Collision Laws, and Some Experimental Data*. PhD thesis, Cornell University, 1997.
- [5] Chatterjee, A. and Ruina, A. Two interpretations of rigidity in rigid body collisions. Accepted for publication in *ASME Journal of Applied Mechanics*, 1998a.
- [6] Chatterjee, A. and Ruina, A. A new algebraic rigid body collision law based on impulse space considerations. Accepted for *ASME Journal of Applied Mechanics*, 1998b.
- [7] Foerster, S. F., Louge, M. Y., Chang, H., and Allia, K. Measurement of the collision properties of small spheres. *Physics of Fluids*, 6(3):1108–1115, 1994.
- [8] Johnson, K. L. *Contact Mechanics*. Cambridge University Press, Cambridge, 1985.
- [9] Kane, T. R. and Levinson, D. A. *Dynamics: Theory and Applications*. McGraw-Hill, New York, 1985.
- [10] Keller, J. B. Impact with friction. *ASME Journal of Applied Mechanics*, 53:1–4, 1986.
- [11] Marghitu, D. B. and Hurmuzlu, Y. Three-dimensional rigid-body collisions with multiple contact points. *ASME Journal of Applied Mechanics*, 62:725–732, 1995.
- [12] Maw, N., Barber, J. R., and Fawcett, J. N. The role of elastic tangential compliance in oblique impact. *Journal of Lubrication Technology*, 103:74–80, 1981.
- [13] R. D. Mindlin and H. Deresiewicz. Elastic spheres in contact under varying oblique forces. *ASME Journal of Applied Mechanics*, 20:327–344, 1953.
- [14] Routh, E. J. *Dynamics of a System of Rigid Bodies*. Macmillan and Co., London, sixth edition, 1897.
- [15] Smith, C. E. Predicting rebounds using rigid-body dynamics. *ASME Journal of Applied Mechanics*, 58:754–758, 1991.
- [16] Smith, C. E. and Liu, P.-P. Coefficients of restitution. *ASME Journal of Applied Mechanics*, 59:963–969, 1992.
- [17] Stoianovici, D. and Hurmuzlu, Y. A critical study of the applicability of rigid-body collision theory. *ASME Journal of Applied Mechanics*, 63:307–316, 1996.
- [18] Stronge, W. J. Planar impact of rough compliant bodies. *International Journal of Impact Engineering*, 15(4):435–450, 1994a.

- [19] Stronge, W. J. Swerve during three-dimensional impact of rough bodies. *ASME Journal of Applied Mechanics*, 61:605–611, 1994b.
- [20] Wang, T. and Mason, M. T. Two-dimensional rigid-body collisions with friction. *ASME Journal of Applied Mechanics*, 59:635–642, 1992.
- [21] Whittaker, E. T. *A Treatise on the Analytical Dynamics of Particles and Rigid Bodies*. Dover, New York, fourth edition, 1944.

## List of Tables

1	Properties of axisymmetric disks used (dimensions in mm, mass in gm, $I_{cm}$ in gm-cm <sup>2</sup> )	11
---	---	----

## List of Figures

1	Axisymmetric delrin disks, with holes or added disks . . . . .	11
2	The coefficient of normal restitution for disks 1 and 2 . . . . .	12
3	Tangential restitution for disks 1 and 2, 4 and 5, 6 and 7. . . . .	13
4	The impulse ratio for disks 1 through 9 . . . . .	14
5	The impulse ratio for all nine disks, The impulse ratio predicted by some collision laws, compared with a bilinear fit to experiment. . . . .	15
6	The impulse ratio for disk 2, for two velocities . . . . .	15

Table 1: Properties of axisymmetric disks used (dimensions in mm, mass in gm,  $I_{cm}$  in gm-cm<sup>2</sup>)

	Disk No.	radius $R$	radius of added disk or hole	thickness	mass $m$	$I$	$2I/mR^2$
Regular	1	49.1	0	6.4	67.8	827	1
	2	49.1	0	6.4	67.2	820	1
With hole	3	49.7	19.7	6.9	59.2	830	1.14
	4	49.6	29.4	6.9	45.4	745	1.33
	5	49.5	29.4	6.9	46.2	761	1.34
With added disk	6	49.1	30.5	6.5	92.0	902	.81
	7	49.2	30.5	6.4	91.5	900	.81
	8	49.2	25.4	6.3	82.8	837	.83
	9	49.1	20.3	6.2	74.6	800	.89

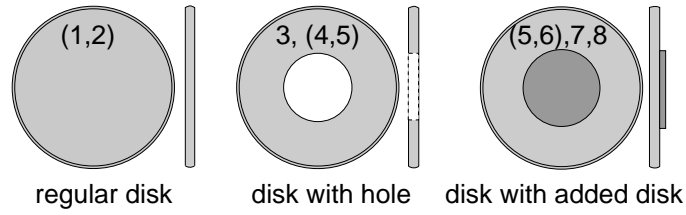


Figure 1: Axisymmetric delrin disks, with holes or added disks

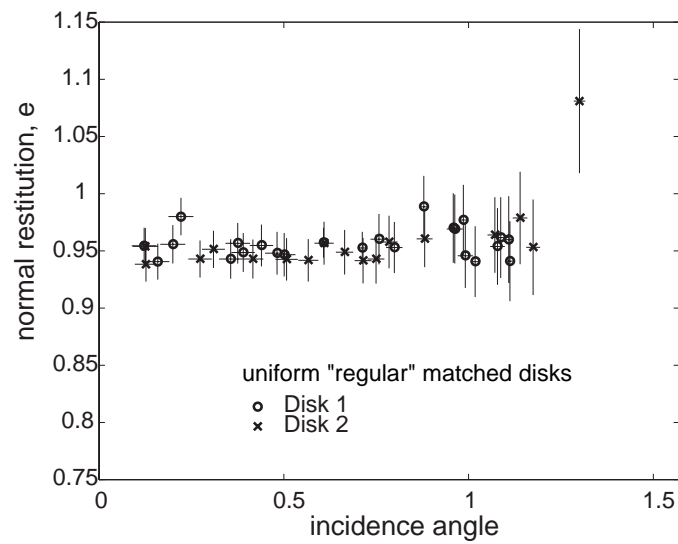


Figure 2: The coefficient of normal restitution for disks 1 and 2

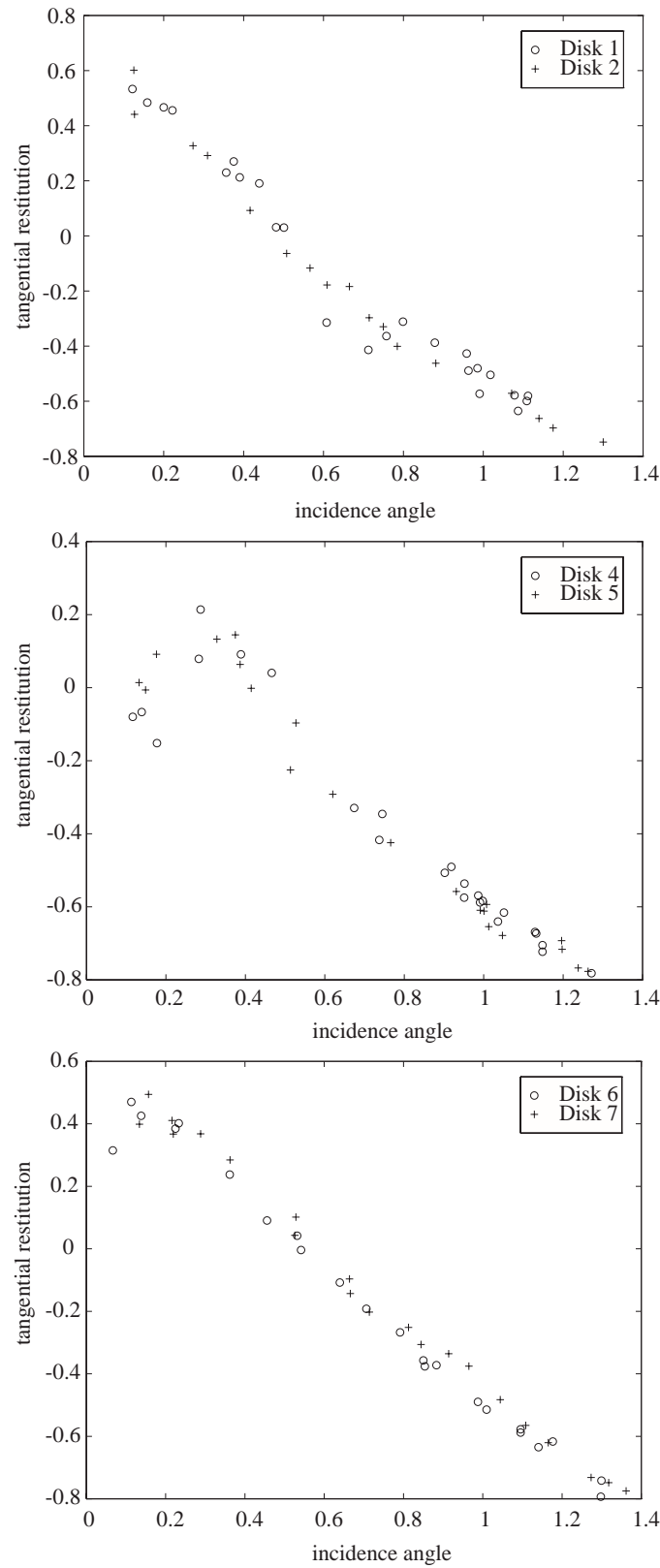


Figure 3: Tangential restitution for disks 1 and 2, 4 and 5, 6 and 7.

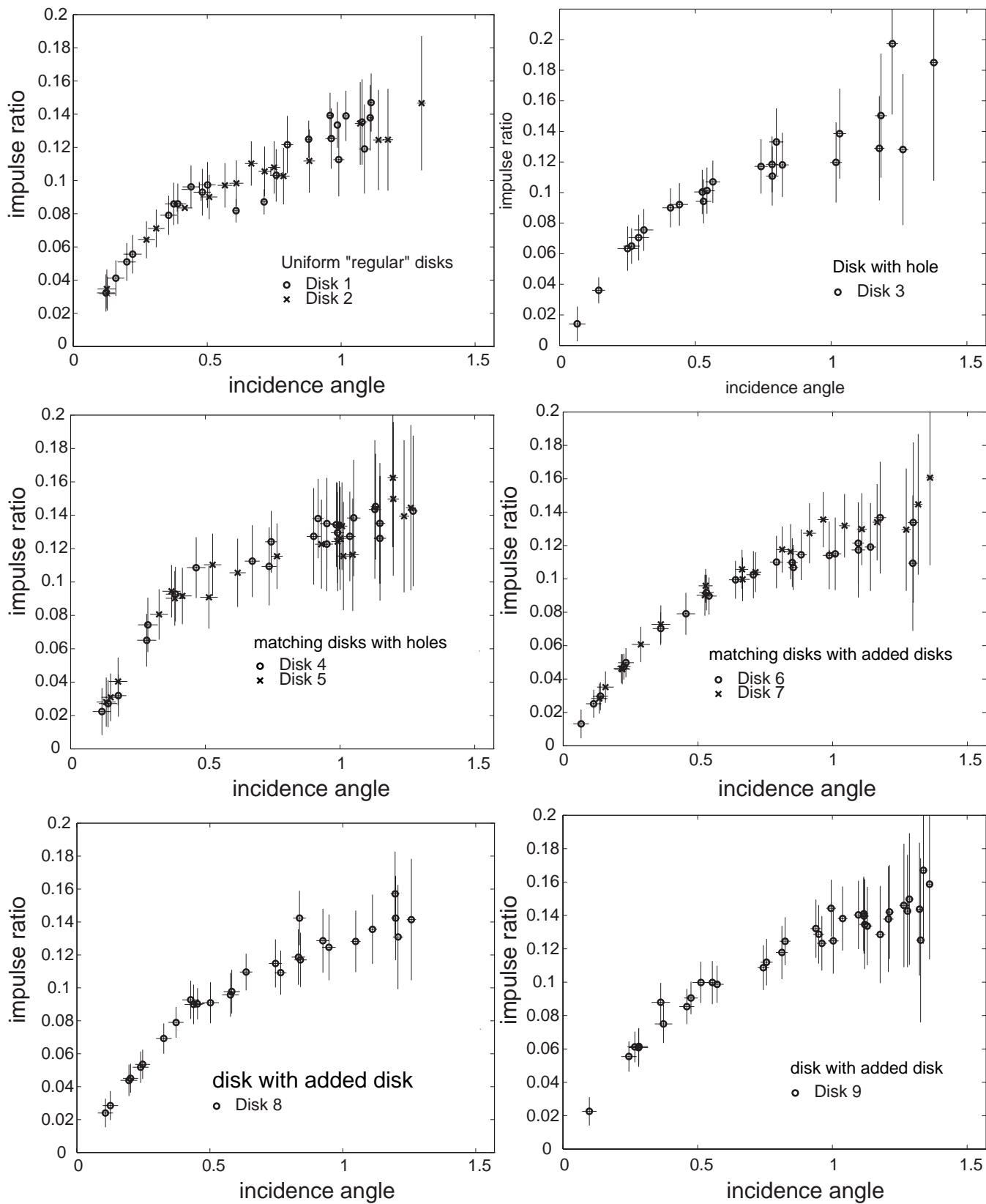


Figure 4: The impulse ratio for disks 1 through 9

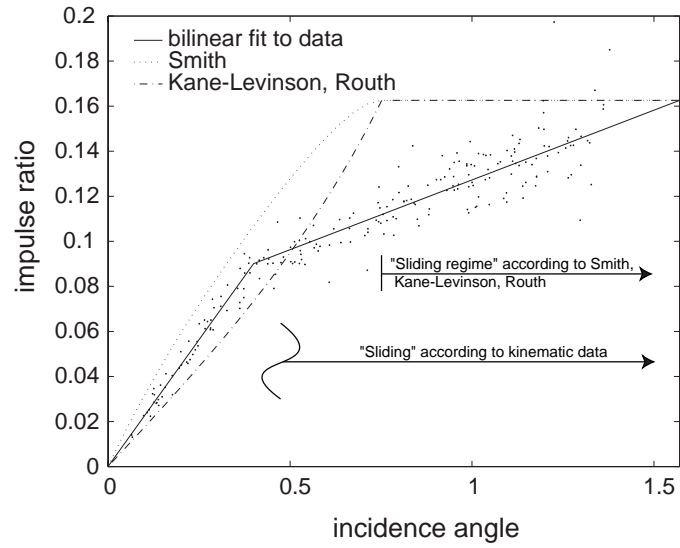


Figure 5: The impulse ratio for all nine disks, The impulse ratio predicted by some collision laws, compared with a bilinear fit to experiment.

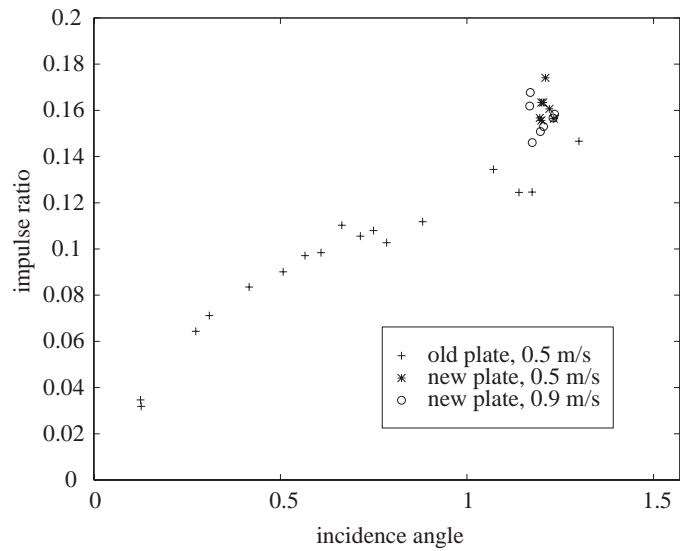


Figure 6: The impulse ratio for disk 2, for two velocities